BNL-211864-2019-JAAM

Surface-to-bulk redox coupling through thermally-driven Li redistribution in Li- and Mn-rich layered cathode materials

S. Li, E. Hu

To be published in "Journal of the American Chemical Society"

July 2019

Chemistry Department

Brookhaven National Laboratory

U.S. Department of Energy

USDOE Office of Energy Efficiency and Renewable Energy (EERE), Vehicle Technologies Office (EE-3V)

DISCLAIMER

Surface-to-bulk redox coupling through thermally-driven Li redistribution in Li- and Mn-rich layered cathode materials

Shaofeng Li[†,‡,▽], Sang-Jun Lee[†,▽], Xuelong Wang[§,⊗], Wanli Yang[#], Hai Huang[†], Daniel S. Swetz[¶], William B. Doriese[¶], Galen C. O'Neil[¶], Joel N. Ullom[¶], Charles J. Titus[‖], Kent D. Irwin[‖], Han-Koo Lee[†,⊥], Dennis Nordlund[†], Piero Pianetta[†], Chang Yu[‡], Jieshan Qiu[‡], Xiqian Yu[⊗], Xiao-Qing Yang[§], Enyuan Hu[*,§], Jun-Sik Lee[*,†], Yijin Liu[*,†]

[†]Stanford Synchrotron Radiation Lightsource, SLAC National Accelerator Laboratory, Menlo Park, CA 94025, USA

[‡]State Key Lab of Fine Chemicals, School of Chemical Engineering, Liaoning Key Lab for Energy Materials and Chemical Engineering, Dalian University of Technology, Dalian 116024, China

[§]Chemistry Division, Brookhaven National Laboratory, Upton, NY 11973, USA

[#]Advanced Light Source, Lawrence Berkeley National Laboratory, Berkeley, CA 94720, USA

[¶]National Institute of Standards and Technology, Boulder, Colorado 80305, USA

[‖]Department of Physics, Stanford University, Stanford, CA 94305, USA

[⊥]Pohang Accelerator Laboratory, Pohang 37673, Republic of Korea

[⊗]Beijing National Laboratory for Condensed Matter Physics, Institute of Physics, Chinese Academy of Sciences, School of Physical Sciences, University of Chinese Academy of Sciences, Beijing 100190, China

KEYWORDS: oxygen activity, redox coupling, Li diffusion, cathode

ABSTRACT: Li- and Mn-rich (LMR) layered cathode materials have demonstrated impressive capacity and specific energy density thanks to their intertwined redox centers including transition metal cations and oxygen anions. Although tremendous efforts have been devoted to the investigation of the electrochemically-driven redox evolution in LMR cathode at ambient temperature, their behavior under a mildly elevated temperature (up to ~100 °C), with or without electrochemical driving force, remains largely unexplored. Here we show a systematic study of the thermally-driven surface-to-bulk redox coupling effect in charged $Li_{1.2}Ni_{0.15}Co_{0.1}Mn_{0.55}O_2$. We for the first time observed a charge transfer between the bulk oxygen anions and the surface transition metal cations under ~100 °C, which is attributed to the thermally-driven redistribution of Li ions. This finding highlights the non-equilibrium state and dynamic nature of the LMR material at deeply delithiated state upon a mild temperature perturbation.

INTRODUCTION

Lithium ion battery (LIB) technology has been widely used to power portable electronics such as laptop computers and smart phones. Recently, the worldwide interest in applying LIB for electric vehicles (EVs), has further sparked enormous research enthusiasm in this field. Considering that fossil fuels account for over 90% of the energy consumed for transportation, the projected boost in the EVs in replacing the internal combustion (IC) engine powered vehicles could have a tremendous market potential and an immense environmental impact.

The energy and power densities of the LIB are two of the most crucial properties for EV application, concerning the cruising distance and the accelerating power, respectively. To achieve the desired improvements in these properties, on the cathode side, a practical approach is to seek for addition redox center that could complement the conventional ones based solely on transition metal (TM) cations. Oxygen redox reaction, at high charging voltage, has been identified as a promising candidate and has attracted a lot of attention.[1-6]

Li- and Mn-rich (LMR) layered materials have been demonstrated as a class of materials with great potential as high energy density battery cathode materials.[7] They are light, inexpensive, and well-performing. It has been demonstrated that the LMR could deliver excellent reversible capacity over 280 mAh g^{-1}. The charge compensation mechanism of LMR involves the synergistic activities of multiple redox centers,[3] including the TM (Mn, Co, and Ni) cations and the oxygen anions. These redox centers are active over different voltage windows and contribute to the overall capacity differently.[3] In particular, the onset charging voltage for the oxygen redox reaction in LMR has been identified to be at over 4.5 V versus Li/Li^+ (**Figure S1**),[1,2] highlighting oxygen anions' role at the deeply delithiated state. While oxygen anions make substantial contributions to the total capacity, they are also the origins of the notorious voltage fade problem and,[8] thus, are currently subjected to intense studies.[9-11] Moreover, the charge transfer among different redox centers could take place in the system, further complicates the reaction mechanism.

Comparing to the amount of efforts that have been devoted into the study of the LIB cathode material's chemical evolution upon electrochemical cycling under ambient temperature, the system's redox behavior under slightly elevated temperature (up to ~100 °C) remains largely unexplored. Although the thermally-driven process under thermal abuse conditions (200 °C and above) is a hot research topic,[12-16] the conventional wisdom holds that the mildly elevated temperature is not enough to induce significant changes. Actually, most of the reported thermally-driven electrode material degradations occur at ~200 °C and above, where the temperature is high enough to provoke mechanical disintegration,[12] unwanted phase transformation,[14] oxygen release,[15] lithium whisker growth,[13] and even thermal runaway.[17-19] These results are valuable in understanding the thermal stability of the cathode materials and safety concerns of the batteries. On the other hand, it is also very important to investigate the cathode materials under mildly elevated temperature (at ~100 °C) because such condition could occurs in liquid LIB, and is definitely required for the operation of solid-state battery with polymer electrolytes.[20] It is also critically important to the initiation of thermal runaway.[18,19] Particularly, for the LMR cathode, the in-depth understanding of the cationic and anionic evolution under such temperature could offer profound insights into the fundamental mechanisms of the charge compensation in the system, which ultimately determines LMR materials' potential as cathode material for both conventional and solid-state LIB.

Here, we have systematically studied the thermally-driven evolution of the LMR cathode at the charged state. We have combined a set of *in-situ* probes including the X-ray imaging, X-ray diffraction, and mass spectrometry to provide complementary insights. These observations suggest that significant lattice transformation, mechanical disintegration, and oxygen release only occurs at thermal abuse conditions at ~200 °C and above, in good agreement with the literature report.[12,13] More thorough study of the LMR cathode's response to the mildly elevated temperature at ~100 °C, was then carried out using advanced soft X-ray spectroscopic tools including a *state-of-the-art* transition edge sensor (TES) spectrometer. Our results suggest that, in the bulk (probing depth at hundreds of nanometers) of the charged LMR cathode, the mild temperature elevation increase the oxidation of the O^{2-} anions but not the TM cations. To compensate for the electron release from the oxygen anions in the bulk, the TM cations (Ni, Mn, and Co) at the particle surface (probing depth at ~5 nm) are found to have lowered valence states compared with the room temperature (RT) sample. Such a surface-to-bulk redox coupling effect is likely caused by the thermally-driven lithium diffusion from the bulk to the surface, resulting in redistribution of Li ions in the LMR cathode material. Such redistribution could have profound consequences on battery operation and safety at elevated temperatures.

RESULTS AND DISCUSSION

For thorough investigation of the thermally-driven chemomechanical transformation in charged LMR materials, we first coupled *in-situ* X-ray imaging and diffraction with mass spectrometry under controlled temperature up to 600 °C. An arbitrarily selected secondary particle, which is recovered from an LMR electrode that was harvested at the fully charged state at 4.8 V, was imaged using the X-ray nano-tomography technique (also known as transmission X-ray microscopy, TXM). As shown in **Figure 1**a, the three-dimensional (3D) rendering and the virtual *xy*-slice through the center of the particle highlight the mesoscale morphological defects that are formed upon electrochemical cycling prior to any thermal treatments.[21-25] We present the morphological comparison between the initial state at room temperature and the state after the particle was exposed to the mildly elevated temperature at ~100 °C for ~5 hours. It appears that there are no detectable changes at this scale. In contrast, further increment of the temperature to ~300 °C over the course of ~2 hours induce noticeable particle fracturing as highlighted by the two red arrows in the right panel of **Figure 1**a.

In general, the morphological degradation at the mesoscale originates from the lattice deformation which would be related with (de)intercalation of the Li ions and/or phase transformation of the hosting material. The lattice deformation leads to the buildup of mechanical stress, which is eventually released through particle cracking.[26,27] As shown in *in-situ* X-ray diffraction (XRD) result (**Figure 1**b), including

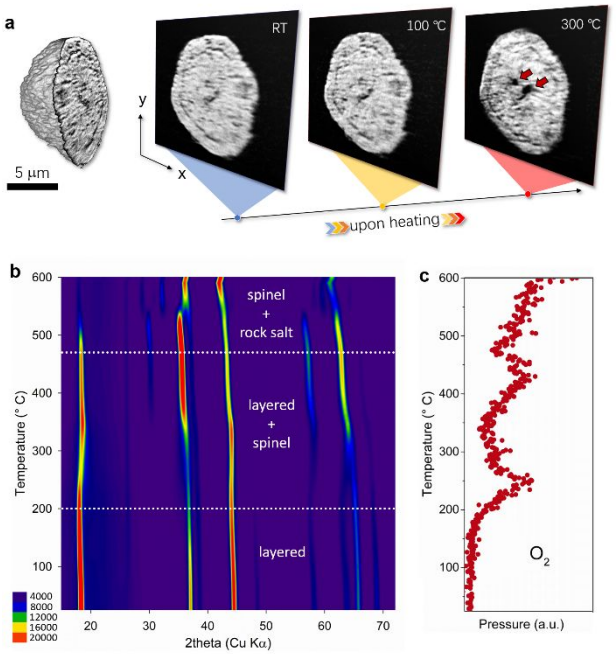

Figure 1. *In-situ* X-ray imaging (a), XRD (b), and mass spectrometry (c) study of charged LMR materials (at 4.8 V) upon exposure to thermal abuse conditions. Significant decomposition of the LMR material is consistently observed near and above ~200 °C.

the high resolution XRD shown in **Figure S2**, the transformation of layered structure to spinel structure starts to take place at ~200 °C in the LMR sample. Further thermal abuse at even higher temperature (~450 °C) is accompanied by the transformation of spinel structure to rock salt structure. These thermally-induced phase transformations at this high temperature are also associated with the molecular oxygen release from the LMR lattice, which is clearly supported by the mass spectrometry data shown in **Figure 1**c. Therefore, based on these bulk-sensitive techniques, we clearly observe that the mesoscale particle fracturing, atomic scale lattice reconstruction, and molecular oxygen release happen concurrently at 200 °C and above.

Compared with the bulk-sensitive techniques, surface-sensitive soft X-ray absorption spectroscopy (XAS) can provide detailed information on the local electronic structure and is sensitive to the oxidation states and chemical bonding. Therefore, we carried out soft XAS measurements at all transition metals (TMs, Ni, Co and Mn) L_3-edges and O *K*-edge on the charged LMR electrode before and after the thermal treatment at ~100 °C for ~5 hours. As shown in **Figure 2**a-c, the TMs L_3-edge XAS spectra, which were measured in the total electron yield (TEY) mode (probing depth at ~5 nm), reveal that the portion of the high valence state of TMs are relatively reduced after heating treatment. The soft XAS spectral at a given element's absorption edge is clearly associated with its valence state.[28] In addition, due to the element's symmetry, the XAS spectrum could exhibit satellite peaks around the absorption energy. The intensity ratio of these multiplet structures is often regarded as a fingerprint of relative oxidation states of the TMs ions.[29-31] Specifically, the high-energy shoulder of Ni L_3-edge decreased and the low-energy shoulders of Co L_3- and Mn L_3-edges increased after the thermal treatment at 100 °C, indicating reduction of TM cations. On the other hand, the TEY signal over the oxygen K-edge remains mostly unchanged after the thermal treatment at 100 °C (**Figure 2**d), which ruled out the the surface reconstruction during the mild thermal treatment. This is because the surface reconstruction will induce significant changes in the O K-edge spectrum. More specifically, the formation of rock-salt/spinel phase would dramatically decrease the intensity of pre-edge peak at ~529.7 eV,[3,32] which is not observed in our study. Therefore, in order to maintain charge neutrality of this system, there must be a charge transfer mechanism between the bulk and the surface of the LMR material.

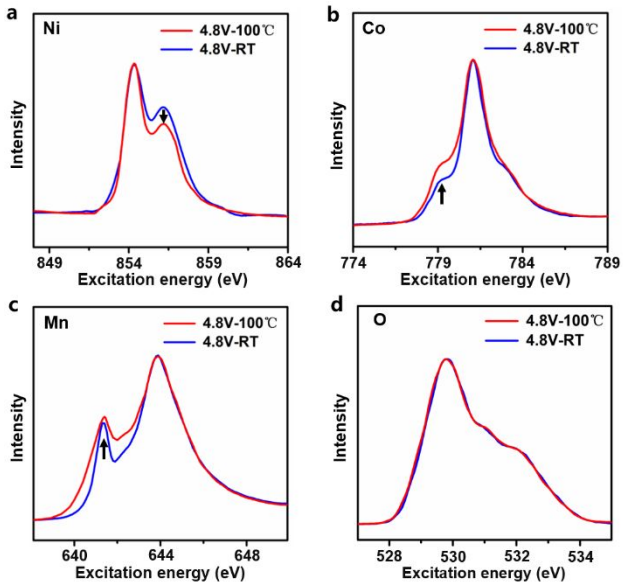

Figure 2. TEY signals from the charged (4.8 V) LMR electrode before and after it is exposed to mildly elevated temperature (100 °C) for ~5 hours. The transition metal elements (Ni, Co, and Mn) appear to be slightly reduced upon heating. All the spectra were normalized at the maximum.

To further elucidate such surface-to-bulk redox coupling effect, we investigate the LMR's spectroscopic fingerprint via the total fluorescence yield (TFY) mode, which probes a few hundred nanometers into the bulk. Note that the TFY signal is often utilized to probe the material's bulk electronic structure. However, it suffers from the competition between the intrinsic absorption efficiency and the penetration depth, leading to severely distorted spectrum shape. And such a distortion is further affected by the intrinsic "self-absorption" effect, which results in stronger fluorescence at higher energies than at the leading-edge energies (**Figure S3**). In particular, the TFY signal over the Mn *L*-edge are the most severely affected. To overcome the self-absorption effect in FY measurement, we must reject unwanted emission lines from the elements other than the targeted one. In other words, we need energy resolving detector. Therefore, we employed a state-of-the-art transition edge sensor (TES) arrays, which is the leading detector technology for nuclear materials analysis, sub-mm and mm-wave astrophysics, and X-ray experiments. The TES detectors are microcalorimeters with intrinsic energy resolution that is sufficient to eliminate the fluorescence background in soft X-ray range. Using advances in SQUID multiplexing technology in TES, SSRL have deployed 240-pixel

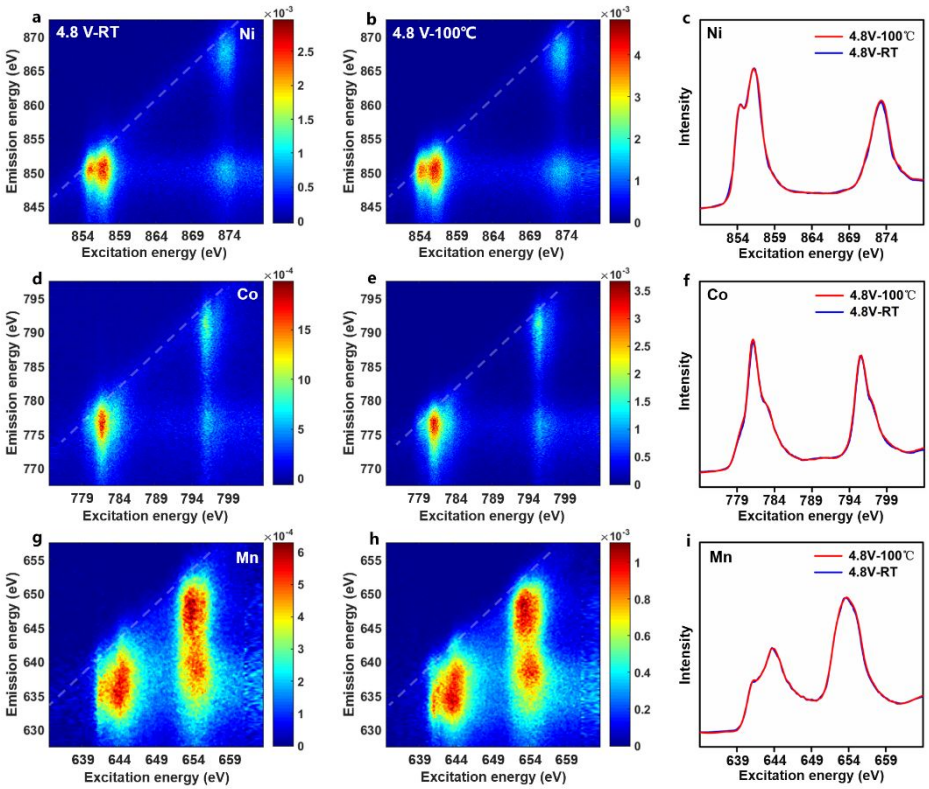

Figure 3. RIXS (left and middle column) and PFY (right column) fingerprints of transition metal elements (Ni (a-c), Co (d-f), and Mn (g-i)) in fully-charged (4.8 V) LMR electrode before and after the thermal treatment at ~100 °C for ~5 hours. Panels (a), (d) and (g) are the RIXS maps collected on the charged LMR electrode under room temperature. Panels (b), (e), and (h) are the RIXS maps collected after the thermal treatment. Panels (c), (f), and (i) are the comparison of PFY signals before and after the thermal treatment. The PFY spectrum is extracted by vertically integrating the signal in corresponding RIXS map. The diagonal white dashed lines in all the RIXS maps are ascribed to the elastic line. No noticeable thermally-induced changes are observed in the RIXS and PFY signatures over the transition metal elements' absorption *L*-edges.

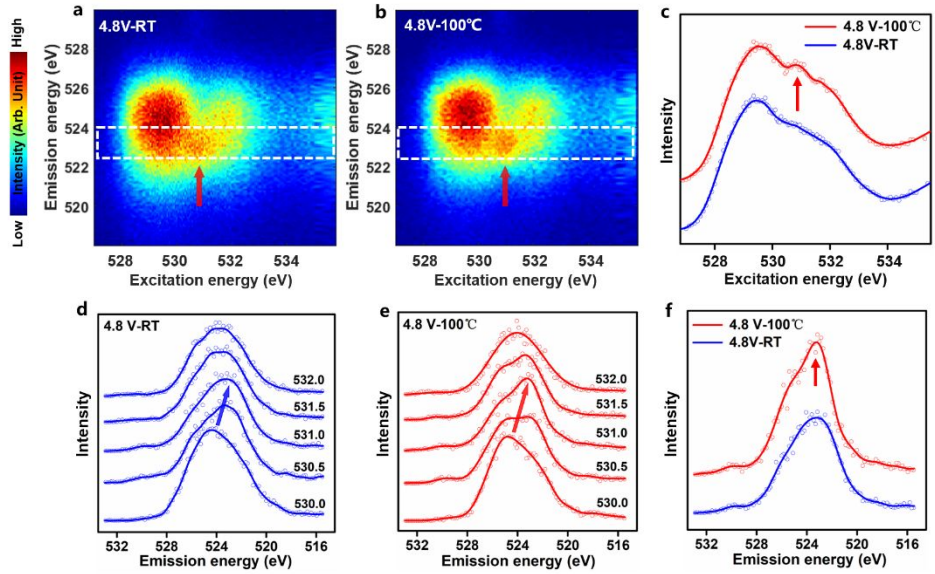

Figure 4. Oxygen RIXS maps from the charged LMR electrode at room temperature (panel (a)) and after thermal treatment at ~100 °C for 5 hours (panel (b)). Panel (c) is the sPFY signal extracted by vertically integrating the signal across a super-partial range marked by the white frames in panels (a) and (b). Panels (d) and (e) are the X-ray emission spectra at selected excitation energy points from 530 to 532 eV in RIXS maps (a) and (b), respectively. Panel (f) is the comparison of the X-ray emission spectra at excitation energy of 531 eV shown in Panel (d) and (e). The formation and enhancement of the RIXS feature at excitation energy of ~531 eV and emission energy of ~523 eV, which is attributed to the oxygen redox reaction, are clearly observed. The solid lines are guide to eyes.

TES array at the beamline 10-1, which has dramatically improved the detection sensitivity.[33]

The TES spectrometer possesses good energy resolution of ~1.4 eV over the energy range that we work with. Therefore, when equipped with a TES spectrometer, the conventional spectroscopic scan could offer valuable insights in the resonant inelastic X-ray scattering (RIXS), partial fluorescence yield (PFY), and X-ray fluorescence (XRF) modalities (see **Figure S4** for an overview of the TES-based spectroscopic data). Specifically, the extraction of PFY signal from the RIXS data greatly enhances the signal-to-noise ratio of the spectra by rejecting unwanted photons that are irrelevant to the targeted signal,[34-37] which carries the bulk signal of the LMR electrode. The comparison of PFY spectra (right column of **Figure 3**) and the TFY spectra (**Figure S3**) clearly features the TES-facilitated data quality improvement. In **Figure 3**, we present the Mn, Co, and Ni $L_{2,3}$-edges RIXS data on the fully-charged LMR electrode before (left column) and after (middle column) the thermal treatment (~100 °C for ~5 hours), which shows no detectable difference. This result clearly indicates that there is no significant valence state deviation of the TMs in bulk of the LMR material upon thermal treatment at ~100 °C. This observation is in good consistency with the implication of **Figure 1**. We note here that the inversed-PFY (iPFY) of the O-*K* emission signal could potentially be used to further avoid the intrinsic self-absorption induced spectrum distortion. The limited signal-to-noise ratio in our data is, unfortunately, insufficient for in-depth analysis of the iPFY data.

Since the valence state of TMs in the bulk of the LMR material demonstrates no change at ~100 °C, the oxygen redox evolution, which has been identified as a key player in the LMR system, becomes the next focus in our search for the charge compensation mechanism for the thermally-driven surface TMs reduction. The oxygen RIXS features have been thoroughly studied and indexed in previous literature.[1,2,38,39] In particular, the oxygen RIXS feature at an excitation energy (i.e., incident photon energy) of ~531 eV and emission energy (emitted photon energy) of ~523 eV is broadly observed and is attributed to the oxygen redox activities. For LMR materials, it has been reported that the formation and evolution of this feature is associated with the deep delithiation of the LMR cathode, which activates oxygen redox reaction at high charging voltage.[1] Note that in **Figure S5**, we systematically compare the oxygen RIXS data from the LMR electrode at pristine state and fully charged state (4.8 V). We clearly observed the formation of the above mentioned RIXS feature when the LMR cathode is charged to 4.8 V. To rule out the contamination of oxygen and TMs signal from the inactive domains (carbon and binder) in the electrode, we also fabricated an electrode without loading of the active LMR particles. This LMR-free electrode has no detectable oxygen RIXS and TMs signal, confirming that the LMR is indeed the sole contributor to the measured signal of oxygen RIXS and TMs L_3-edge spectra. Therefore, our result confirms that, at high state of charge (SoC), the lattice oxygen redox reaction in LMR material is activated and is a major charge compensation mechanism for the deep delithiation of the LMR cathode.

More interestingly, the comparison of the oxygen RIXS data before and after the thermal treatment of charged LMR electrode (**Figure 4**) suggests that the oxygen redox activity is enhanced even after a mild temperature treatment (~100 °C). On the one hand, the super-partial fluorescence yields (sPFY) signal[28] was extracted by vertically integrating the signal across a super-partial range marked by the white frames in **Figure 4**a and b. It is clearly observed that the intensity of the oxygen RIXS feature at an excitation energy of ~531 eV is enhanced after thermal treatment at 100 °C (**Figure 4**c). Further comparison of the normalized sPFY spectra shown in **Figure S6** clearly confirmed this result. On the other hand, as shown in **Figure 4**d and e, we extract the X-ray emission spectra (XES) at a few selected excitation energies from 530 to 532 eV from the oxygen RIXS maps. In addition to the visualization of the XES evolution, we highlight the comparision of the XES at an emission energy of ~523 eV in **Figure 4**f, which further confirms the enhaced oxygen redox reaction after the thermal treatment at 100 °C. All of these results together suggest the thermally-promoted transformation of O^{2-} to oxygen with higher valence state (O^{-}) in the bulk of the LMR cathode. In other words, mildly elevated temperature could enhance the oxygen activity in the LMR lattice and, thus, favor the oxygen redox through previously proposed mechanisms like the formation of O-O dimers,[40] localized oxygen holes,[9] or other specific oxygen chemical bonds.[10] The oxidation of the oxygen anions in the bulk is, therefore, the charge compensation mechanism for the reduction of TMs on the surface at ~100 °C. Such a surface-to-bulk redox coupling between the TMs cations and oxygen anions is likely resulted from the thermally driven Li ions diffusion within the LMR lattice, which motivates a more thorough investigation of the lithium diffusivity in the LMR material.

Galvanostatic intermittent titration technique (GITT), an effective electrochemical method to calculate the lithium diffusion coefficient, is employed in this work. The experimental details are described in the method section and the analysis follows that proposed by Weppner and Huggins.[41] The GITT curve of LMR material during the 1st cycle charging is shown in **Figure 5**a with the inset graph illustrating how the voltage evolves during a titration step.

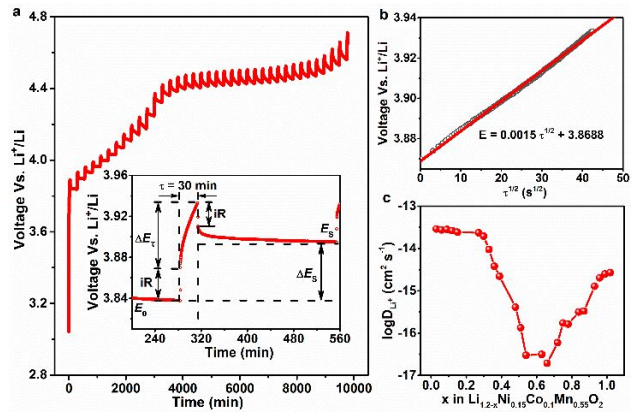

Figure 5. GITT measurement of LMR and the computed lithium diffusivity during charging. (a) Voltage profile during the GITT experiment with the inset graph showing how voltage evolves during a titration step. The meanings of the variables are described in the text. (b) The linear relationship between voltage and the square root of τ during the voltage increase stage when the current is applied. (c) Li ion diffusivity evolution during the first cycle charging process of LMR material.

Specifically, upon a pulse charging, the voltage is immediately increased by iR, in which i is the current and R is the resistance, respectively. Then the voltage slowly increases, due to the galvanostatic charge pulse, in order to maintain a constant concentration gradient. When the charging current is stopped, the voltage is immediately decreased by iR. Then the voltage slowly decreases as lithium is diffused in the bulk until an equilibrium is reached in the system. By measuring various voltage increases or drops during the titration process and using the following equation, Li^+ diffusion coefficient can be calculated:[42]

$$D_{Li^+} = \frac{4}{\pi}\left(\frac{m_B V_M}{M_B S}\right)^2 \left(\frac{\Delta E_S}{\tau\left(dE_\tau / d\sqrt{\tau}\right)}\right)^2 \left(\tau \ll \frac{L^2}{D_{Li^+}}\right) \quad (1)$$

where m_B is the mass of the active material in the electrode, V_M is the molar volume, M_B is the molecular weight of LMR material, S is the active surface area of the electrode whose value is based on Brunauer, Emmett, and Teller (BET) result,[43] τ is the time duration in which the current is applied, and L is the thickness of the electrode. If E_τ and $\tau^{1/2}$ follow a linear relationship as shown in **Figure 5**b, equation (1) can be further simplified into:

$$D_{Li^+} = \frac{4}{\pi\tau}\left(\frac{m_B V_M}{M_B S}\right)^2 \left(\frac{\Delta E_S}{\Delta E_\tau}\right)^2 \quad (2)$$

The calculated lithium diffusion coefficients during 1st cycle charging of LMR material is shown in **Figure 5**c. It shows that at the beginning of charging, D_{Li^+} is on the order of 10^{-14} cm^2 s^{-1} which is in good agreement with results in the literature.[42,44] When more than 0.3 Li is extracted from the lattice, a sharp decrease in D_{Li^+} is observed, with several orders of magnitude change (the y axis is $\log_{10} D_{Li^+}$). A minimum in D_{Li^+} is reached (on the order of 10^{-17}) when around 0.7 Li is extracted. After that, D_{Li^+} increases but remains much lower than the initial stage of charging. Such results indicate that Li^+ transport properties deteriorates significantly in LMR material during the 1st cycle charging. Moreover, the galvanostatic oxidization curve (normal charging curve at a rate of C/8) is overlay on the GITT results as shown in **Figure S7**. At the late stage of charging, normal charging curve deviates significantly from the open-circuit-voltage (OCV) determined by GITT experiment, suggesting that Li^+ diffusion kinetics are so slow that it requires considerable amount of time for the system to reach equilibrium (as indicated by the OCV). This can induce a large Li concentration gradient within the particle if a relatively large current is applied for charging as in the case of normal operation. Consequently, the chemical potential of Li in the bulk is likely to be higher than that near the surface, creating thermodynamic driving force for the Li ions to migrate when the particle is relaxed. Such Li migration is believed to be the root cause of the observed surface-to bulk redox coupling phenomenon. There is a known hysteresis effect in the cycling of LMR cathode. Upon charging, the TMs undergo redox reaction at relatively lower state of charge and the oxygen takes over at more deeply delithiated state. However, when discharging the cell, the TM reduction actually happens in the early stage of the discharging.[1,45] Oxygen oxidization immediately followed by transition metal reduction during electrochemical cycling suggests that these two processes are close in free energy (in LMR materials). A slight temperature elevation as in our case can change the weight of enthalpy term and entropy term (magnified by temperature), potentially leading to a change of sequence in the greatness of free energy. It is also should be noted that, the crystalline phase of the fully charged LMR materials remains unchanged after the thermal treatment at 100 °C (**Figure S2**). It indicates that these migrated lithium ions are from lithium layer rather than the transition metal layer.

As schematically shown in **Figure 6**, at the charged state, the LMR cathode likely exhibits a lithium concentration gradient (with higher lithium concentration in the bulk and lower lithium concentration on the surface) due to the limited lithium diffusivity in LMR lattice. Starting from such ununiform distribution of lithium, the mild temperature perturbation promotes the lithium mobility and causes the system to rearrange as it settles to a new equilibrium. In this scenario, thermally-promoted ionic mobility in the hosting LMR lattice could facilitate the surface-to-bulk redox coupling effect and maximizes the entropy of the system. As discussed, a mild temperature elevation to nearly ~100 °C can commonly occur in liquid LIB. More importantly, such a thermal condition is definitely required for the operation of solid-state battery with polymer electrolytes, which constitutes one of the major frontier research directions for the next generation LIB. On the other hand, the mildly elevated temperature could improve the specific capacity for the LMR material to some content, which has been reported in the literature.[46] The fundamental mechanism of the temperature effect on LMR's electrochemical performance is, however, not yet clear. Based on our results, the thermally enhanced lithium diffusivity should be the root cause of the observed surface-to-bulk redox coupling effect, which would ultimately suppress the charge heterogeneity in the LMR cathode. Such a charge heterogeneity is generally undesirable because it could lead to a series of chemomechanical events that are harmful to the system at different length scales.[47] Therefore, our study of the LMR's redox evolution under mild temperature perturbation highlights the surface-to-bulk redox coupling, which could potentially impact the LMR cathode's performance positively.

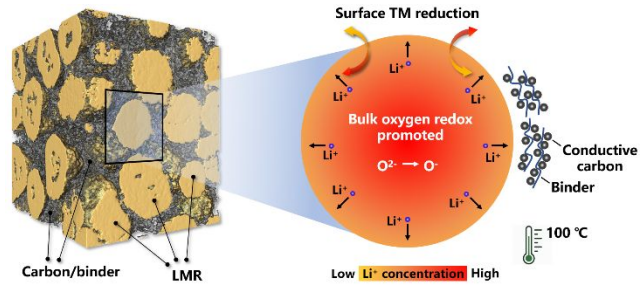

Figure 6. Schematic illustration of the observed thermally promoted redox coupling effect. The mild temperature elevation to 100 °C triggers the charge transfer between the oxygen anions in the bulk and the transition metal cations on the particle surface through activation of the lithium ion diffusion.

CONCLUSION

In this work, we employed a series of *in-situ* experimental techniques to investigate the charged LMR cathode's response to elevated temperature. It was clearly observed that the mesoscale particle fracturing, atomic scale lattice reconstruction, and molecular oxygen release happen concurrently at 200 °C and above. More importantly, combined with the advanced soft XAS tools, including a *state-of-the-art* TES spectrometer, we discovered that the oxygen redox activity in the bulk of LMR material is promoted under 100 °C, compensating the TM reduction on the surface. Such a surface-to-bulk redox coupling effect is attributed to the thermally-driven lithium diffusion from the bulk to the surface. This work presents a fundamental understanding of the redox-coupling effect in LMR cathode under mildly elevated temperature. The methodology developed herein also pave a new way towards the investigation of LIB materials behavior under practical conditions with industrial relevance.

ASSOCIATED CONTENT

Supporting Information.
The Supporting Information is available free of charge via the Internet at http://pubs.acs.org."
Detailed experimental description, supporting figures (PDF)

AUTHOR INFORMATION

Corresponding Author

*enhu@bnl.gov
*jslee@slac.stanford.edu
*liuyijin@slac.stanford.edu

Author Contributions

[▽]S. Li and S.-J. Lee contributed equally to this work.

Notes

The authors declare no competing financial interest.

ACKNOWLEDGMENT

Use of the Stanford Synchrotron Radiation Lightsource, SLAC National Accelerator Laboratory, is supported by the U.S. Department of Energy (DOE), Office of Science, Office of Basic Energy Sciences under Contract No. DE-AC02-76SF00515. The work done at Brookhaven National Laboratory was supported by the Assistant Secretary for Energy Efficiency and Renewable Energy, Vehicle Technology Office of the U.S. DOE through the Advanced Battery Materials Research (BMR) Program, including Battery500 Consortium under contract No. DE-SC0012704. This research used beamline 7-BM of the National Synchrotron Light Source II, a U.S. DOE Office of Science User Facility operated for the DOE Office of Science by Brookhaven National Laboratory under Contract No. DE-SC0012704. This research used beamline 17BM of the Advanced Photon Source, a U.S. DOE Office of Science User Facility operated for the DOE Office of Science by Argonne National Laboratory under Contract No. DE-AC02-06CH11357. S. Li acknowledges the support from the Chinese Scholarship Council (No. 201806060018). The engineering support from D. Van Campen, D. Day and V. Borzenets for the TXM experiment at beamline 6-2C of SSRL is gratefully acknowledged.

REFERENCES

(1) Gent, W. E.; Lim, K.; Liang, Y.; Li, Q.; Barnes, T.; Ahn, S. J.; Stone, K. H.; McIntire, M.; Hong, J.; Song, J. H.; Li, Y.; Mehta, A.; Ermon, S.; Tyliszczak, T.; Kilcoyne, D.; Vine, D.; Park, J. H.; Doo, S. K.; Toney, M. F.; Yang, W.; Prendergast, D.; Chueh, W. C. Coupling between oxygen redox and cation migration explains unusual electrochemistry in lithium-rich layered oxides. *Nat. Commun.* **2017**, *8*, 2091.

(2) Xu, J.; Sun, M.; Qiao, R.; Renfrew, S. E.; Ma, L.; Wu, T.; Hwang, S.; Nordlund, D.; Su, D.; Amine, K.; Lu, J.; McCloskey, B. D.; Yang, W.; Tong, W. Elucidating anionic oxygen activity in lithium-rich layered oxides. *Nat. Commun.* **2018**, *9*, 947.

(3) Hu, E.; Yu, X.; Lin, R.; Bi, X.; Lu, J.; Bak, S.; Nam, K.-W.; Xin, H. L.; Jaye, C.; Fischer, D. A.; Amine, K.; Yang, X.-Q. Evolution of redox couples in Li- and Mn-rich cathode materials and mitigation of voltage fade by reducing oxygen release. *Nat. Energy* **2018**, *3*, 690.

(4) Assat, G.; Tarascon, J.-M. Fundamental understanding and practical challenges of anionic redox activity in Li-ion batteries. *Nat. Energy* **2018**, *3*, 373.

(5) Xie, Y.; Saubanère, M.; Doublet, M. L. Requirements for reversible extra-capacity in Li-rich layered oxides for Li-ion batteries. *Energy Environ. Sci.* **2017**, *10*, 266.

(6) Sathiya, M.; Rousse, G.; Ramesha, K.; Laisa, C. P.; Vezin, H.; Sougrati, M. T.; Doublet, M. L.; Foix, D.; Gonbeau, D.; Walker, W.; Prakash, A. S.; Ben Hassine, M.; Dupont, L.; Tarascon, J. M. Reversible anionic redox chemistry in high-capacity layered-oxide electrodes. *Nat. Mater.* **2013**, *12*, 827.

(7) Yang, F.; Liu, Y.; Martha, S. K.; Wu, Z.; Andrews, J. C.; Ice, G. E.; Pianetta, P.; Nanda, J. Nanoscale morphological and chemical changes of high voltage lithium-manganese rich NMC composite cathodes with cycling. *Nano Lett.* **2014**, *14*, 4334.

(8) Croy, J. R.; Balasubramanian, M.; Gallagher, K. G.; Burrell, A. K. Review of the U.S. department of energy's "deep five" effort to understand voltage fade in Li- and Mn-rich cathodes. *Acc. Chem. Res.* **2015**, *48*, 2813.

(9) Luo, K.; Roberts, M. R.; Hao, R.; Guerrini, N.; Pickup, D. M.; Liu, Y. S.; Edstrom, K.; Guo, J.; Chadwick, A. V.; Duda, L. C.; Bruce, P. G. Charge-compensation in 3d-transition-metal-oxide intercalation cathodes through the generation of localized electron holes on oxygen. *Nat. Chem.* **2016**, *8*, 684.

(10) Seo, D.-H.; Lee, J.; Urban, A.; Malik, R.; Kang, S.; Ceder, G. The structural and chemical origin of the oxygen redox activity in layered and cation-disordered Li-excess cathode materials. *Nat. Chem.* **2016**, *8*, 692.

(11) Maitra, U.; House, R. A.; Somerville, J. W.; Tapia-Ruiz, N.; Lozano, J. G.; Guerrini, N.; Hao, R.; Luo, K.; Jin, L.; Pérez-Osorio, M. A.; Massel, F.; Pickup, D. M.; Ramos, S.; Lu, X.; McNally, D. E.; Chadwick, A. V.; Giustino, F.; Schmitt, T.; Duda, L. C.; Roberts, M. R.; Bruce, P. G. Oxygen redox chemistry without excess alkali-metal ions in $Na_{2/3}[Mg_{0.28}Mn_{0.72}]O_2$. *Nat. Chem.* **2018**, *10*, 288.

(12) Yan, P.; Zheng, J.; Chen, T.; Luo, L.; Jiang, Y.; Wang, K.; Sui, M.; Zhang, J. G.; Zhang, S.; Wang, C. Coupling of electrochemically triggered thermal and mechanical effects to aggravate failure in a layered cathode. *Nat. Commun.* **2018**, *9*, 2437.

(13) Wei, C.; Zhang, Y.; Lee, S.-J.; Mu, L.; Liu, J.; Wang, C.; Yang, Y.; Doeff, M.; Pianetta, P.; Nordlund, D.; Du, X.-W.; Tian, Y.; Zhao, K.; Lee, J.-S.; Lin, F.; Liu, Y. Thermally driven mesoscale chemomechanical interplay in $Li_{0.5}Ni_{0.6}Mn_{0.2}Co_{0.2}O_2$ cathode materials. *J. Mater. Chem. A* **2018**, *6*, 23055.

(14) Mu, L.; Yuan, Q.; Tian, C.; Wei, C.; Zhang, K.; Liu, J.; Pianetta, P.; Doeff, M. M.; Liu, Y.; Lin, F. Propagation topography of redox phase transformations in heterogeneous layered oxide cathode materials. *Nat. Commun.* **2018**, *9*, 2810.

(15) Mu, L.; Lin, R.; Xu, R.; Han, L.; Xia, S.; Sokaras, D.; Steiner, J. D.; Weng, T.-C.; Nordlund, D.; Doeff, M. M.; Liu, Y.; Zhao, K.; Xin,

H. L.; Lin, F. Oxygen release induced chemomechanical breakdown of layered cathode materials. *Nano Lett.* **2018**, *18*, 3241.
(16) Hu, E.; Bak, S.-M.; Liu, Y.; Liu, J.; Yu, X.; Zhou, Y.-N.; Zhou, J.; Khalifah, P.; Ariyoshi, K.; Nam, K.-W.; Yang, X.-Q. Utilizing environmental friendly iron as a substitution element in spinel structured cathode materials for safer high energy lithium-ion batteries. *Adv. Energy Mater.* **2016**, *6*, 1501662.
(17) Finegan, D. P.; Scheel, M.; Robinson, J. B.; Tjaden, B.; Hunt, I.; Mason, T. J.; Millichamp, J.; Di Michiel, M.; Offer, G. J.; Hinds, G.; Brett, D. J. L.; Shearing, P. R. In-operando high-speed tomography of lithium-ion batteries during thermal runaway. *Nat. Commun.* **2015**, *6*, 6924.
(18) Finegan, D. P.; Darcy, E.; Keyser, M.; Tjaden, B.; Heenan, T. M. M.; Jervis, R.; Bailey, J. J.; Malik, R.; Vo, N. T.; Magdysyuk, O. V.; Atwood, R.; Drakopoulos, M.; DiMichiel, M.; Rack, A.; Hinds, G.; Brett, D. J. L.; Shearing, P. R. Characterising thermal runaway within lithium-ion cells by inducing and monitoring internal short circuits. *Energy Environ. Sci.* **2017**, *10*, 1377.
(19) Finegan, D. P.; Darcy, E.; Keyser, M.; Tjaden, B.; Heenan, T. M. M.; Jervis, R.; Bailey, J. J.; Vo, N. T.; Magdysyuk, O. V.; Drakopoulos, M.; Di Michiel, M.; Rack, A.; Hinds, G.; Brett, D. J. L.; Shearing, P. R. Identifying the cause of rupture of Li-ion batteries during thermal runaway. *Adv. Sci.* **2018**, *5*, 1700369.
(20) Besli, M. M.; Xia, S.; Kuppan, S.; Huang, Y.; Metzger, M.; Shukla, A. K.; Schneider, G.; Hellstrom, S.; Christensen, J.; Doeff, M. M.; Liu, Y. Mesoscale chemomechanical interplay of the $LiNi_{0.8}Co_{0.15}Al_{0.05}O_2$ cathode in solid-state polymer batteries. *Chem. Mater.* **2019**, *31*, 491.
(21) Mao, Y.; Wang, X.; Xia, S.; Zhang, K.; Wei, C.; Bak, S.; Shadike, Z.; Liu, X.; Yang, Y.; Xu, R.; Pianetta, P.; Ermon, S.; Stavitski, E.; Zhao, K.; Xu, Z.; Lin, F.; Yang, X.-Q.; Hu, E.; Liu, Y. High-voltage charging-induced strain, heterogeneity, and micro-cracks in secondary particles of a nickel-rich layered cathode material. *Adv. Funct. Mater.* **2019**, *29*, 1900247.
(22) Wei, C.; Xia, S.; Huang, H.; Mao, Y.; Pianetta, P.; Liu, Y. Mesoscale battery science: the behavior of electrode particles caught on a multispectral X-ray camera. *Acc. Chem. Res.* **2018**, *51*, 2484.
(23) Liu, H.; Wolf, M.; Karki, K.; Yu, Y.-S.; Stach, E. A.; Cabana, J.; Chapman, K. W.; Chupas, P. J. Intergranular cracking as a major cause of long-term capacity fading of layered cathodes. *Nano Lett.* **2017**, *17*, 3452.
(24) Tsai, P.-C.; Wen, B.; Wolfman, M.; Choe, M.-J.; Pan, M. S.; Su, L.; Thornton, K.; Cabana, J.; Chiang, Y.-M. Single-particle measurements of electrochemical kinetics in NMC and NCA cathodes for Li-ion batteries. *Energy Environ. Sci.* **2018**, *11*, 860.
(25) Wang, J.; Chen-Wiegart, Y.-c. K.; Wang, J. In situ three-dimensional synchrotron X-ray nanotomography of the (de)lithiation processes in tin anodes. *Angew. Chem. Int. Ed.* **2014**, *53*, 4460.
(26) Xu, R.; de Vasconcelos, L. S.; Shi, J.; Li, J.; Zhao, K. Disintegration of meatball electrodes for $LiNi_xMn_yCo_zO_2$ cathode materials. *Exp. Mech.* **2018**, *58*, 549.
(27) Xia, S.; Mu, L.; Xu, Z.; Wang, J.; Wei, C.; Liu, L.; Pianetta, P.; Zhao, K.; Yu, X.; Lin, F.; Liu, Y. Chemomechanical interplay of layered cathode materials undergoing fast charging in lithium batteries. *Nano Energy* **2018**, *53*, 753.
(28) de Groot, F. M. F.; Fuggle, J. C.; Thole, B. T.; Sawatzky, G. A. 2p x-ray absorption of 3d transition-metal compounds: An atomic multiplet description including the crystal field. *Phys. Rev. B* **1990**, *42*, 5459.
(29) Liu, X.; Liu, J.; Qiao, R.; Yu, Y.; Li, H.; Suo, L.; Hu, Y.-s.; Chuang, Y.-D.; Shu, G.; Chou, F.; Weng, T.-C.; Nordlund, D.; Sokaras, D.; Wang, Y. J.; Lin, H.; Barbiellini, B.; Bansil, A.; Song, X.; Liu, Z.; Yan, S.; Liu, G.; Qiao, S.; Richardson, T. J.; Prendergast, D.; Hussain, Z.; de Groot, F. M. F.; Yang, W. Phase transformation and lithiation effect on electronic structure of Li_xFePO_4: an in-depth study by soft X-ray and simulations. *J. Am. Chem. Soc.* **2012**, *134*, 13708.
(30) Lin, F.; Nordlund, D.; Li, Y.; Quan, M. K.; Cheng, L.; Weng, T.-C.; Liu, Y.; Xin, H. L.; Doeff, M. M. Metal segregation in hierarchically structured cathode materials for high-energy lithium batteries. *Nat. Energy* **2016**, *1*, 15004.
(31) Wu, J.; Song, J.; Dai, K.; Zhuo, Z.; Wray, L. A.; Liu, G.; Shen, Z.-x.; Zeng, R.; Lu, Y.; Yang, W. Modification of Transition-Metal Redox by Interstitial Water in Hexacyanometalate Electrodes for Sodium-Ion Batteries. *J. Am. Chem. Soc.* **2017**, *139*, 18358.
(32) Tian, C.; Nordlund, D.; Xin, H. L.; Xu, Y.; Liu, Y.; Sokaras, D.; Lin, F.; Doeff, M. M. Depth-dependent redox behavior of $LiNi_{0.6}Mn_{0.2}Co_{0.2}O_2$. *J. Electrochem. Soc.* **2018**, *165*, A696.
(33) Titus, C. J.; Baker, M. L.; Lee, S. J.; Cho, H.-M.; Doriese, W. B.; Fowler, J. W.; Gaffney, K.; Gard, J. D.; Hilton, G. C.; Kenney, C.; Knight, J.; Li, D.; Marks, R.; Minitti, M. P.; Morgan, K. M.; O'Neil, G. C.; Reintsema, C. D.; Schmidt, D. R.; Sokaras, D.; Swetz, D. S.; Ullom, J. N.; Weng, T.-C.; Williams, C.; Young, B. A.; Irwin, K. D.; Solomon, E. I.; Nordlund, D. L-edge spectroscopy of dilute, radiation-sensitive systems using a transition-edge-sensor array. *J. Chem. Phys.* **2017**, *147*, 214201.
(34) Achkar, A. J.; Regier, T. Z.; Wadati, H.; Kim, Y. J.; Zhang, H.; Hawthorn, D. G. Bulk sensitive X-ray absorption spectroscopy free of self-absorption effects. *Phys. Rev. B* **2011**, *83*, 081106.
(35) Qiao, R.; Wray, L. A.; Kim, J.-H.; Pieczonka, N. P. W.; Harris, S. J.; Yang, W. Direct experimental probe of the Ni(II)/Ni(III)/Ni(IV) redox evolution in $LiNi_{0.5}Mn_{1.5}O_4$ electrodes. *J. Phys. Chem. C* **2015**, *119*, 27228.
(36) Qiao, R.; Li, Q.; Zhuo, Z.; Sallis, S.; Fuchs, O.; Blum, M.; Weinhardt, L.; Heske, C.; Pepper, J.; Jones, M.; Brown, A.; Spucces, A.; Chow, K.; Smith, B.; Glans, P.-A.; Chen, Y.; Yan, S.; Pan, F.; Piper, L. F. J.; Denlinger, J.; Guo, J.; Hussain, Z.; Chuang, Y.-D.; Yang, W. High-efficiency in situ resonant inelastic x-ray scattering (iRIXS) endstation at the Advanced Light Source. *Rev. Sci. Instrum.* **2017**, *88*, 033106.
(37) Dai, K.; Wu, J.; Zhuo, Z.; Li, Q.; Sallis, S.; Mao, J.; Ai, G.; Sun, C.; Li, Z.; Gent, W. E.; Chueh, W. C.; Chuang, Y.-d.; Zeng, R.; Shen, Z.-x.; Pan, F.; Yan, S.; Piper, L. F. J.; Hussain, Z.; Liu, G.; Yang, W. High reversibility of lattice oxygen redox quantified by direct bulk probes of both anionic and cationic redox reactions. *Joule* **2019**, *3*, 518.
(38) Wu, J.; Li, Q.; Sallis, S.; Zhuo, Z.; Gent, E. W.; Chueh, C. W.; Yan, S.; Chuang, Y.-d.; Yang, W. Fingerprint oxygen redox reactions in batteries through high-efficiency mapping of resonant inelastic X-ray scattering. *Condens. Matter* **2019**, *4*, 5.
(39) Yang, W.; Devereaux, T. P. Anionic and cationic redox and interfaces in batteries: advances from soft X-ray absorption spectroscopy to resonant inelastic scattering. *J. Power Sources* **2018**, *389*, 188.
(40) McCalla, E.; Abakumov, A. M.; Saubanère, M.; Foix, D.; Berg, E. J.; Rousse, G.; Doublet, M.-L.; Gonbeau, D.; Novák, P.; Van Tendeloo, G.; Dominko, R.; Tarascon, J.-M. Visualization of O-O peroxo-like dimers in high-capacity layered oxides for Li-ion batteries. *Science* **2015**, *350*, 1516.
(41) Weppner, W.; Huggins, R. A. Determination of the kinetic parameters of mixed-conducting electrodes and application to the system Li_3Sb. *J. Electrochem. Soc.* **1977**, *124*, 1569.
(42) Li, Z.; Du, F.; Bie, X.; Zhang, D.; Cai, Y.; Cui, X.; Wang, C.; Chen, G.; Wei, Y. Electrochemical kinetics of the $Li[Li_{0.23}Co_{0.3}Mn_{0.47}]O_2$ cathode material studied by GITT and EIS. *J. Phys. Chem. C* **2010**, *114*, 22751.
(43) Nanda, J.; Martha, S. K.; Kalyanaraman, R. High-capacity electrode materials for electrochemical energy storage: role of nanoscale effects. *Pramana* **2015**, *84*, 1073.
(44) Yu, H.; Wang, Y.; Asakura, D.; Hosono, E.; Zhang, T.; Zhou, H. Electrochemical kinetics of the $0.5Li_2MnO_3{\cdot}0.5LiMn_{0.42}Ni_{0.42}Co_{0.16}O_2$ 'composite' layered

cathode material for lithium-ion batteries. *RSC Adv.* **2012**, *2*, 8797.
(45) Gallagher, K. G.; Croy, J. R.; Balasubramanian, M.; Bettge, M.; Abraham, D. P.; Burrell, A. K.; Thackeray, M. M. Correlating hysteresis and voltage fade in lithium- and manganese-rich layered transition-metal oxide electrodes. *Electrochem. Commun.* **2013**, *33*, 96.
(46) Yu, H.; So, Y.-G.; Ren, Y.; Wu, T.; Guo, G.; Xiao, R.; Lu, J.; Li, H.; Yang, Y.; Zhou, H.; Wang, R.; Amine, K.; Ikuhara, Y. Temperature-sensitive structure evolution of lithium-manganese-rich layered oxides for lithium-ion batteries. *J. Am. Chem. Soc.* **2018**, *140*, 15279.
(47) Yang, Y.; Xu, R.; Zhang, K.; Lee, S.-J.; Mu, L.; Liu, P.; Waters, C. K.; Spence, S.; Xu, Z.; Wei, C.; Kautz, D. J.; Yuan, Q.; Dong, Y.; Yu, Y.-S.; Xiao, X.; Lee, H.-K.; Pianetta, P.; Cloetens, P.; Lee, J.-S.; Zhao, K.; Lin, F.; Liu, Y. Quantification of heterogeneous degradation in Li-ion batteries. *Adv. Energy Mater.* **2019**, 1900674.